

# Study of Catalytic Properties of Aluminophosphates with Different Phase Compositions

O. V. KIKHTYANIN, E. A. PAUKSHTIS, K. G. IONE, AND V. M. MASTIKHIN

*Institute of Catalysis, 6300-0 Novosibirsk 90, Prospekt Akademika Lavrentieva, 5, USSR*

Received September 29, 1988; revised March 20, 1990

Aluminophosphates  $\text{AlPO}_4\text{-}5$  distinguished by the time of their crystallization have been prepared and their properties have been investigated by XRD, IRS, and NMR methods and catalytic testing. The catalyst selectivity in methanol conversion depends on the preparation. It is suggested that the catalytic properties of aluminophosphates  $\text{AlPO}_4\text{-}5$  are connected with the state and environment of the Al atoms. © 1990 Academic Press, Inc.

## INTRODUCTION

A new class of compounds with a unique microporous framework, aluminophosphates of the  $\text{AlPO}_4\text{-}n$  type, can be used as adsorbents and catalysts (1, 2). Unlike aluminosilicates, a number of which are found in nature, the aluminophosphate molecular sieves are synthesized by hydrothermal treatment of an aluminophosphate gel formed by mixing of the sources of aluminium and phosphorus with an organic template. In most cases hydrated aluminium oxide (pseudo-boehmite form) is used as the source of aluminium. During crystallization of  $\text{AlPO}_4\text{-}n$  species the composition of the solid reaction product is varied from aluminium oxide through amorphous aluminophosphate to a regular microporous structure in which Al and P atoms of the framework have tetrahedral coordination by O atoms. The adsorptive and catalytic properties of these compounds are different, as the nature and the concentration of active sites in the samples are changed. In this work we show the dependence of physicochemical properties of aluminophosphates  $\text{AlPO}_4\text{-}5$  on their phase composition. Catalytic properties in methanol conversion of the aluminophosphates as well as atomic states have been investigated by catalytic testing and NMR and IRS methods.

## EXPERIMENTAL

### 1. Synthesis of $\text{AlPO}_4\text{-}5$ Aluminophosphates

The samples were prepared by hydrothermal treatment ( $T_{\text{cryst.}} = 200^\circ\text{C}$ ; time of crystallization was varied from 0.5 to 20 h) of aluminophosphate gels of composition 1.0  $\text{Al}_2\text{O}_3$ :1.0  $\text{P}_2\text{O}_5$ :1.5  $(\text{C}_2\text{H}_5)_3\text{N}$ :40  $\text{H}_2\text{O}$  formed by mixing of orthophosphoric acid (85% wt) and hydrated aluminium oxide (pseudo-boehmite form, 76% wt  $\text{Al}_2\text{O}_3$ ) in the presence of triethylamine. The solid reaction product was recovered by filtration from a steel pressure vessel lined with an inert plastic material, washed with water, dried in air at room temperature, and then calcined at 550–600°C.

### 2. X-Ray Diffraction Analysis

XRD analysis was carried out on an automatic diffractometer with monochromatic  $\text{CuK}\alpha$  irradiation in the range  $2\theta = 4\text{--}40^\circ$ . The degrees of crystallinity of the samples were determined using reflections in the range  $2\theta = 18\text{--}24^\circ$ .

### 3. NMR Studies

The  $^{27}\text{Al}$  and  $^{31}\text{P}$  NMR spectra were recorded on a Bruker CXP-300 spectrometer with magic angle spinning. For  $^{27}\text{Al}$  NMR spectra the  $\text{Al}(\text{H}_2\text{O})_6^{3+}$  aquacomplex was taken as a reference (resonance frequency

78.18 MHz); for  $^{31}\text{P}$  NMR spectra, 85% orthophosphoric acid (121.45 MHz).

#### 4. IRS Studies

IR spectra were recorded with a UR-20 spectrometer. The properties of acid sites of the catalysts were determined from carbon monoxide, pyridine, and ammonia adsorption using an assumption of proportionality of concentration of acid sites and intensity of corresponding absorption bands (3). The data on integral absorption coefficients were used when studying CO adsorption (4). Concentrations of Brønsted sites were calculated from pyridine adsorption using the intensity of the  $1540\text{-cm}^{-1}$  band for  $\text{PyH}^+$  ions and the  $1450\text{-cm}^{-1}$  band for  $\text{Py}:\text{Al}^{3+}$  complexes with coefficients taken from Refs. (5, 6).

#### 5. Methanol Conversion Studies

Catalytic testing was carried out with a pulsed gradientless installation at a reaction temperature of  $500^\circ\text{C}$ . The volume concentration of methanol in the reaction mixture was 12–15% and the contact time was  $1 \pm 0.1$  s. Helium was used as the carrier gas. The reaction products were analyzed by gas chromatography.

### RESULTS

X-ray spectra of the aluminophosphates contain reflections which belong to the

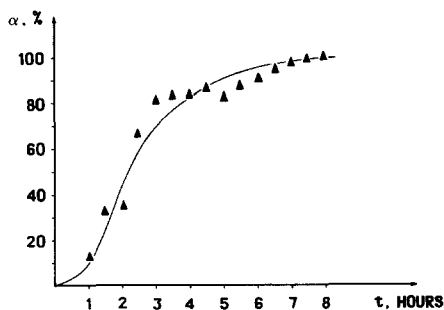


FIG. 1. Influence of crystallization time ( $t$ ) of aluminophosphate gel on the content of  $\text{AlPO}_4\text{-5}$  phase in the crystallization product ( $\alpha$ , %).  $T_{\text{cryst.}} = 200^\circ\text{C}$ ,  $\text{Al}_2\text{O}_3:\text{P}_2\text{O}_5 = 1$  in the initial mixture; 1- $\alpha$ , amorphous phase.

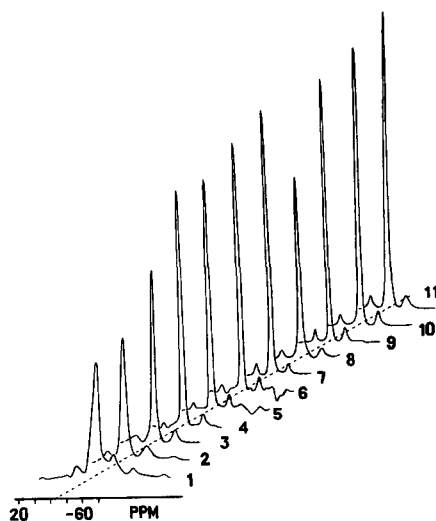


FIG. 2.  $^{31}\text{P}$  NMR spectra of aluminophosphates. 1, A-1; 2, A-1.5; 3, A-2; 4, A-2.5; 5, A-3; 6, A-3.5; 7, A-4; 8, A-4.5; 9, A-5; 10, A-5.5; 11, A-6.

$\text{AlPO}_4\text{-5}$  structure only, the degree of crystallinity depending on the time of crystallization of the aluminophosphate gel (Fig. 1). The  $\text{AlPO}_4\text{-5}$  phase begins to form 1 h after the beginning of hydrothermal treatment of the reaction mixture. More than 6 h of crystallization time does not essentially change the degree of crystallinity of the samples.

In  $^{31}\text{P}$  NMR, spectra signals with chemical shifts at  $-26$ – $-32$  ppm are observed which, according to Ref. (7), correspond to P atoms in tetrahedral coordination with P–O–Al bonds (Fig. 2, Table 1).  $^{27}\text{Al}$  NMR spectra show that Al atoms in the samples can be in both octahedral and tetrahedral coordination (Fig. 3, Table 1). In agreement with Ref. (8), signals with  $\delta = -1 \pm 2$  ppm belong to Al atoms in octahedral coordination in aluminium oxide, signals with  $\delta$  in the range  $-12$ – $-20$  ppm belong to Al atoms in octahedral coordination in aluminophosphates, and signals with  $\delta$  in the range  $31$ – $36$  ppm belong to Al atoms in tetrahedral coordination in aluminophosphates. From the data in Table 1 and Figs. 2 and 3, it can be seen that with increasing crystallization time of the aluminophosphate gel, signal in-

TABLE 1

Chemical Composition and Chemical Shifts in NMR Spectra of Aluminophosphate Catalysts

Sample	Chemical composition (mol, $\pm 2\%$ )	$\delta^{27}\text{Al}$ (ppm, $\pm 2$ ppm)		$\delta^{31}\text{P}$ (ppm, $\pm 2$ ppm)	$\frac{I_{\text{Al-oct. Al}_2\text{O}_3}}{I_{\text{Al-oct. AlPO}_4}}$ ( $\pm 20\%$ )	$\frac{I_{\text{Al-oct. AlPO}_4}}{I_{\text{Al-tetr. AlPO}_4}}$ ( $\pm 20\%$ )
		Tetrahedral	Octahedral			
A-1	$\text{Al}_2\text{O}_3 : 0.31 \text{ P}_2\text{O}_5$	36.8, 58	0	-26.5	2.3	0.45
A-1.5	$\text{Al}_2\text{O}_3 : 0.46 \text{ P}_2\text{O}_5$	33.1	-1.2, -18	-30.5	0.54	0.49
A-2	$\text{Al}_2\text{O}_3 : 0.60 \text{ P}_2\text{O}_5$	31.2	2.5, -16.2	-30.5, -22	0.25	0.48
A-2.5	$\text{Al}_2\text{O}_3 : 0.89 \text{ P}_2\text{O}_5$	33.1	1.8, -11.8	-30.5	0.4	0.22
A-3	$\text{Al}_2\text{O}_3 : 0.95 \text{ P}_2\text{O}_5$	33.1	-16.2	-30.5	0	0.20
A-3.5	$\text{Al}_2\text{O}_3 : 0.92 \text{ P}_2\text{O}_5$	31.2	-16.2	-30.5	0	0.19
A-4	$\text{Al}_2\text{O}_3 : 0.98 \text{ P}_2\text{O}_5$	31.8	-16.8	-31.3	0	0.14
A-4.5	$\text{Al}_2\text{O}_3 : 1.04 \text{ P}_2\text{O}_5$	32.4	-15	-31.3	0	0.13
A-5	$\text{Al}_2\text{O}_3 : 1.02 \text{ P}_2\text{O}_5$	32.5	-16.3	-29.7, -32.1	0	0.08
A-5.5	$\text{Al}_2\text{O}_3 : 1.02 \text{ P}_2\text{O}_5$	32.7	-17.3	-29.7, -32.1	0	0.07
A-6	$\text{Al}_2\text{O}_3 : 1.01 \text{ P}_2\text{O}_5$	32.5	—	-31.3	0	0

tensity in the range  $-1$ – $+2$  ppm continually decreases and signal intensity in the range  $31$ – $36$  ppm increases. Samples A-1–A-4 have signals in the range  $-1$ – $-20$  ppm with the greatest intensities. In the spectrum of the A-1 sample there is a signal with a chemical shift of  $58$  ppm which belongs to Al atoms in tetrahedral coordination in aluminium oxide.

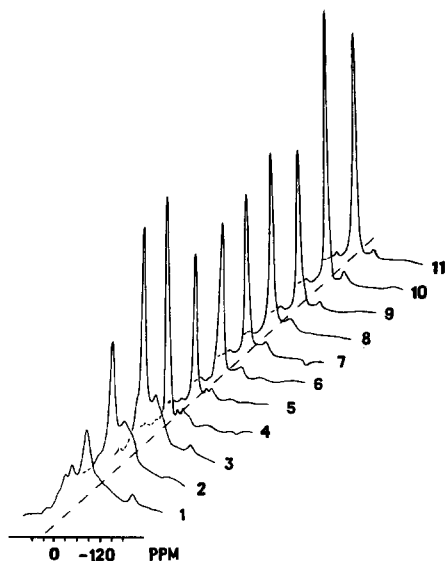


FIG. 3.  $^{27}\text{Al}$  NMR spectra. The designations are the same as those in Fig. 2.

The results of IRS studies are presented in Tables 2 and 3 and in Figs. 4–6. The  $3675\text{-cm}^{-1}$  band belongs to P–OH groups (9); the weak band at  $3790\text{-cm}^{-1}$  belongs to Al–OH groups with Al atoms in tetrahedral coordination (10); and a broad band at  $3730$ – $3740\text{-cm}^{-1}$  is characteristic of Al–OH groups in aluminium oxide where Al atoms are in octahedral coordination. Changes in intensities of the signals in this region for A-1–A-3 samples are small. The A-6 sample is distinguished by decreased concentrations of P–OH and Al–OH groups. In addition to the OH groups mentioned, the IR spectra of the samples have a broad band at  $3450$ – $3500$

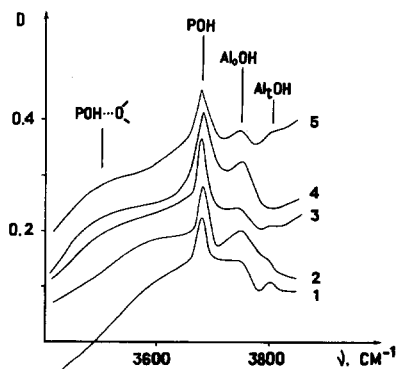


FIG. 4. IR spectra of OH groups of aluminophosphates. 1, A-1; 2, A-1.5; 3, A-2; 4, A-3; 5, A-6.

TABLE 2  
Main Characteristics of Acid Sites in Aluminophosphates

Sample	Characteristics of OH groups		Characteristics of Brønsted sites		Characteristics of Lewis sites		
	$I_{\text{OH}3675}$ ( $\text{cm}^{-1}/\text{g}$ , $\pm 15\%$ )	$I_{\text{OH}3730-3740}$ (arbitr. units/g, $\pm 15\%$ )	$I_{\text{NH}_4^+}$ ( $\text{cm}^{-1}/\text{g}$ , $\pm 15\%$ )	$N_{\text{PyH}^+}$ ( $\mu\text{mol/g}$ , $\pm 25\%$ )	$N_{\text{CO}}(\nu_{\text{CO}})$ ( $\mu\text{mol/g}$ , $\pm 25\%$ )	$N_{\text{Py}}(\nu_{\text{CCN}})$ ( $\mu\text{mol/g}$ , $\pm 25\%$ )	$I_{\text{NH}_3:\text{Al}}$ ( $\nu = 1330$ ) (arbitr. units/g, $\pm 15\%$ )
A-1	200	3	260	35	100(2192)	110(1613)	12
A-1.5	160	5.6	540	22	72(2192)	63(1617)	5
A-2	155	3.3	550	22	61(2200)	51(1616)	3
A-3	180	4.0	640	30	41(2200)	51(1616)	4
A-6	130	1.6	930	18	Traces	0	1

$\text{cm}^{-1}$ . The study of acidic properties of the OH groups at  $3675 \text{ cm}^{-1}$  by displacement of  $\nu_{\text{OH}}$  by hydrogen bonding with CO ( $\Delta\nu_{\text{OH}} = 150\text{--}165 \text{ cm}^{-1}$ ), according to Ref. (11), gave values of PA (proton affinity) of these OH groups ( $1290 \pm 20 \text{ kJ/mol}$ ).

Studies of pyridine adsorption on aluminophosphates have indicated the presence of both Brønsted ( $\nu = 1540 \text{ cm}^{-1}$ ) and Lewis ( $\nu = 1450 \text{ cm}^{-1}$ ) acid sites (12) (Table 2). The same sites, Brønsted and Lewis, are identified by IR spectra of adsorbed ammonia (Fig. 5, Table 2). Lewis sites appear as complexes with ammonia characterized by bands at  $1620 \text{ cm}^{-1}$  (it is not shown in Fig. 5 since the position of the band is not associ-

ated with the properties of the complex) and by bands below  $1350 \text{ cm}^{-1}$  (12). There is an intensive absorption by  $\text{PO}_4$  tetrahedra of the framework of the catalysts ( $\nu \sim 1200 \text{ cm}^{-1}$ ) (9) that obscures lower frequency bands.

Ammonium ions are identified from the appearance of broad bands at  $1400\text{--}1500 \text{ cm}^{-1}$  (Fig. 5). The intensity of these bands changes independently of the intensity of

TABLE 3  
Concentrations of Acid Sites of Catalysts on Surfaces of  $\text{Al}_2\text{O}_3$  and  $\text{AlPO}_4$  Phases

Sample	Content of Lewis acid sites ( $\mu\text{mol/g}$ , $\pm 25\%$ )			
	$N_{\text{CO}}$		$N_{\text{Py}}$	
	$\text{Al}_2\text{O}_3$	$\text{AlPO}_4$	$\text{Al}_2\text{O}_3$	$\text{AlPO}_4$
A-1	90	10	99	11
A-1.5	49	23	43	20
A-2	30	31	25	26
A-3	0	41	0	51
A-6	0	0	0	0

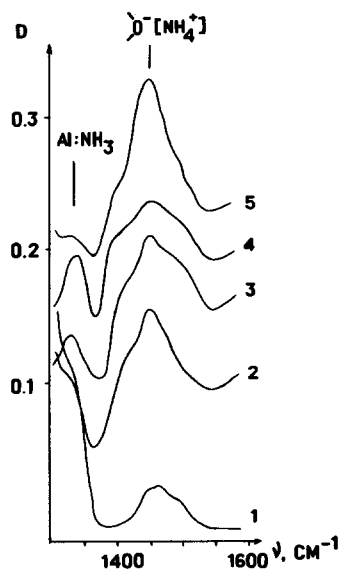


FIG. 5. IR spectra observed during ammonia adsorption. The designations are the same as those in Fig. 4.

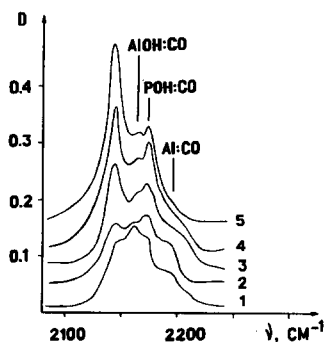


FIG. 6. IR spectra of CO adsorbed on aluminophosphates. The designations are the same as those in Fig. 4.

the band at  $3675\text{ cm}^{-1}$  (Fig. 4) and increases from the A-1 to the A-6 sample.

The IR spectra of adsorbed CO have a number of bands (Fig. 6) which can be attributed to complexes resulting from interaction of CO with Brønsted and Lewis sites. The bands at  $2172\text{ cm}^{-1}$  (P-OH $\cdot\cdot$ CO) and  $2163\text{ cm}^{-1}$  (Al-OH $\cdot\cdot$ CO) are attributed to -OH:CO complexes. These conclusions were made from a comparison of the data obtained with those of CO adsorption on  $\text{Al}_2\text{O}_3$  (13) and  $\text{H}_3\text{PO}_4/\text{SiO}_2$ . An intensive band at  $2142\text{ cm}^{-1}$  is also present in the spectra. Its position almost coincides with  $\nu_{\text{CO}}$  in the gas phase ( $\nu = 2145\text{ cm}^{-1}$ ) (14) and its intensity increases as the number of samples grows from A-1 to A-6. It is possible that this intensive band is caused by a large amount of physically adsorbed CO in the channels of the framework. Bonds corresponding to  $\text{Al}^{3+}:\text{CO}$  complexes are displayed in the spectra of A-1-A-3 samples. Table 2 contains the characteristics of these Lewis sites. The concentration of the sites decreases invariably from A-1 to A-3 samples. The strength of the sites (on the scale of CO adsorption heat (15) increases from 33 to 37 kJ/mol when passing from A-1-A-1.5 to A-2-A-3 samples. Almost the same data are obtained by studying the pyridine adsorption on the catalysts (Table 2). The concentration of the sites decreases from A-1 to A-3 samples, and strength, eval-

uated qualitatively from  $\nu_{(\text{CCN})}$ , increases from A-1 to A-3 samples. The change in intensity of the band corresponding to coordinated ammonia ( $\nu = 1330\text{ cm}^{-1}$ ) in arbitrary units confirms the conclusion made for pyridine and CO adsorption on aluminophosphates also. Moreover, the change in the shape of the band at  $1300\text{--}1350\text{ cm}^{-1}$ , which is attributed to  $\text{NH}_3:\text{Al}^{3+}$  complexes, indicates the displacement of the band from A-1-A-1.5 to A-2-A-6 samples to the range of higher frequencies and, hence, the growth in strength of Lewis sites (12).

Table 4 indicates the data on catalytic testing on aluminophosphates. It is seen that selectivity of the catalysts toward the products of methanol decomposition (CO and  $\text{CH}_4$ ) decreases while that toward dimethyl ether (DME) increases when passing from A-1 to A-6. A-3 has the highest selectivity toward hydrocarbons  $\text{C}_2^+$  including aromatics.

#### DISCUSSION

Aluminophosphates with microporous structures are formed through the mixing of aluminium oxide and phosphoric acid followed by crystallization of this reaction mixture under hydrothermal conditions. The data in Table 1 indicate that relative intensities of signals in the  $^{27}\text{Al}$  NMR spectra from Al atoms in octahedral and tetrahedral coordinations in the  $\text{Al}_2\text{O}_3$  phase decrease with increasing crystallization time of the sam-

TABLE 4

Catalytic Properties of Aluminophosphates in Methanol Conversion ( $T_{\text{reac.}} = 500^\circ\text{C}$ )

Sample	Methanol conversion (% , $\pm 2\%$ )	Selectivity (% wt., $\pm 2\%$ )		
		DME	CO + $\text{CH}_4$	Hydrocarbons $\text{C}_2^+$
A-1	97.1	5.0	85.9	9.1
A-1.5	96.1	34.4	28.7	36.9
A-2	95.5	35.0	17.3	47.7
A-3	94.8	11.9	7.7	80.4
A-6	78.0	97.8	1.4	0.8

ples, and the relative intensities of signals from Al atoms in octahedral coordination in an  $\text{AlPO}_4$  phase have a small maximum owing to the beginning of  $\text{AlPO}_4$ -5 structure formation. The catalysts obtained have different phase compositions, i.e., different ratios of  $\text{Al}_2\text{O}_3$ ,  $\text{AlPO}_4$ -5, and amorphous aluminophosphate phases in solid reaction products. The compositions of active sites of the samples were investigated by IR spectroscopy, an assumption being taken into account that for all the samples the  $\text{Al}_2\text{O}_3$ / $\text{AlPO}_4$  phase ratio, i.e., the states of Al atoms in  $\text{Al}_2\text{O}_3$  and  $\text{AlPO}_4$  phases, exert an identical influence on the sets of experimental data obtained in both NMR and IRS studies. An attempt was undertaken to determine independently the concentrations of acidic sites in  $\text{Al}_2\text{O}_3$  and  $\text{AlPO}_4$  phases. The fact was taken into consideration that per 1 g of the sample the concentration of Lewis sites in aluminium oxide is at least four times higher than that in amorphous  $\text{AlPO}_4$  (16). Concentrations of acidic sites for A-1–A-6 catalysts calculated for  $\text{Al}_2\text{O}_3$  and  $\text{AlPO}_4$  phases separately are presented in Table 3. These data indicate that an increased concentration of Lewis acid sites for the  $\text{AlPO}_4$  amorphous phase (as  $\text{AlPO}_4$ -5 phase does not include octahedrally coordinated Al atoms and, hence, Lewis acid sites) in the samples A-2–A-3 are observed.

DME is the first product of methanol conversion on acid–base catalysts (17). Further hydrocarbons  $\text{C}_2^+$  can be formed on strong acid sites or the reaction may proceed through the decomposition of DME to CO and  $\text{CH}_4$  (18). In the latter case coordinatively unsaturated Al atoms in octahedral coordination in the  $\text{Al}_2\text{O}_3$  phase can serve as active sites (17). In our case the relation between the presence of  $\text{Al}_2\text{O}_3$  phase in the samples and their selectivity toward methanol decomposition products is observed (Fig. 7). In the  $^{27}\text{Al}$  NMR spectra of highly crystalline samples, the  $I_{\text{Al-oct. AlPO}_4}/I_{\text{Al-tetr. AlPO}_4}$  ratio is close to zero, indicating that almost all the Al atoms are in the regular  $\text{AlPO}_4$ -5 framework. The IRS study shows that such

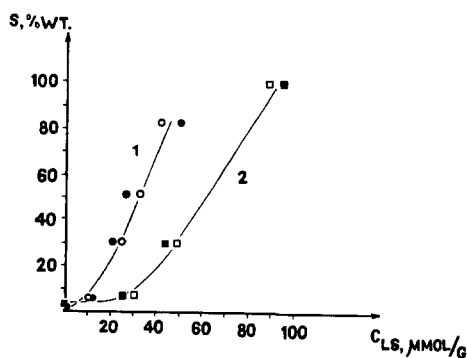


FIG. 7. Influence of concentration of Lewis acid sites in  $\text{Al}_2\text{O}_3$  (○) and  $\text{AlPO}_4$  (●) phases determined from CO (□) and pyridine (■) adsorption on selectivity of catalysts toward hydrocarbons (1) and products of methanol decomposition (2).  $T_{\text{reac.}} = 500^\circ\text{C}$ .

samples do not possess Lewis acid sites and their acidity is caused by the presence of Al–OH and P–OH groups, the strength of which is insufficient for methanol conversion to hydrocarbons  $\text{C}_2^+$ . The only reaction product on highly crystalline samples is DME and selectivity of aluminophosphates toward hydrocarbons  $\text{C}_2^+$  depends on the presence of Al atoms in octahedral coordination in  $\text{AlPO}_4$  phase (Fig. 7). Thus, we suppose that hydrocarbon formation on the samples is realized with the participation of Al atoms in octahedral coordination to O atoms in the  $\text{AlPO}_4$  phase; however, the role of Brønsted sites may be important also. The transition of Al atoms in octahedral coordination from the  $\text{Al}_2\text{O}_3$  phase to the  $\text{AlPO}_4$  phase causes alteration of selectivity of the samples through the changes brought about by the surrounding of these atoms and their coordinative saturation.

The different behavior of the signals in IR spectra of the catalysts from those of OH groups ( $\nu = 3675\text{ cm}^{-1}$ ) and ammonium ions when the number of the samples is increased may be explained by the presence of a bond with  $\nu = 3450\text{--}3500\text{ cm}^{-1}$  (Fig. 4) in IR spectra of the OH groups. The intensity of this bond increases from A-1 to A-6, and it can probably be attributed to bound P–OH groups in the channels of the structure (of

type P-OH...O ). Adsorbed ammonia forms ammonium ions on such groups, also leading to an increase in bond intensity over that of ammonium ions for A-1.5-A-6 samples. On the other hand, the data from Table 2 show that bond intensity from OH groups ( $\nu = 3675 \text{ cm}^{-1}$ ) correlates with pyridinium ion formation, and this permits us to assume the absence of interaction between  $\text{PyH}^+$  ions and bounded P-OH groups. In all probability, these groups are inaccessible for rather large molecules; thus the first stage of methanol conversion, i.e., DME formation, proceeds on unbonded, terminal P-OH groups, corresponding to the  $\nu = 3675 \text{ cm}^{-1}$  bond. Correlation between the decrease in intensity of the latter bond and the decrease in methanol conversion when the number of the samples is increased (Table 4) confirms this supposition.

#### CONCLUSION

The selectivity of aluminophosphates in methanol conversion is determined by the concentration of Brønsted and Lewis acid sites in the catalyst. In its turn, the type of active sites depends on the phase composition of aluminophosphates and finally on the time of crystallization of the catalysts.

DME formation from methanol occurs on highly crystalline samples with participation of terminal P-OH groups, but hydrocarbon formation does not take place on these samples. This is evidence that such catalysts have no strong acid sites. Decomposition of methanol into CO and  $\text{CH}_4$  occurs on the samples which contain the sites with octahedrally coordinated Al atoms in  $\text{Al}_2\text{O}_3$  phase, while DME dehydration to hydrocarbons  $\text{C}_2^+$  proceeds with the participation of octa-

hedrally coordinated Al atoms in  $\text{AlPO}_4$  phase. However, the role of Brønsted acid sites in this case may also be significant. The data obtained in this work confirm our supposition (18) that, in aluminophosphates with microporous structures, active sites of hydrocarbon formation from methanol include Al atoms in octahedral coordination.

#### REFERENCES

1. US Patent No. 4310440 (1982).
2. Flanigen, E. M., Lok, B. M., Patton, R. L., and Wilson, S. T., in "Proceedings, 7th Intern. Zeolite Conf., Tokyo," Vol. 103, 1986.
3. Paukshtis, E. A., Soltanov, R. I., and Yurchenko, E. N., *React. Kinet. Catal. Lett.* **23**, 333 (1983).
4. Soltanov, R. I., Paukshtis, E. A., and Yurchenko, E. N., *Kinet. Katal.* **23**, 164 (1982).
5. Hughes, T. R., and White, H. M., *J. Phys. Chem.* **71**, 2192 (1967).
6. Paukshtis, E. A., Soltanov, R. I., and Yurchenko, E. N., *React. Kinet. Catal. Lett.* **19**, 119 (1982).
7. Müller, D., Jahn, E., Ladvig, G., and Haubenreisser, U. M., *Chem. Phys. Lett.* **109**, 332 (1984).
8. Müller, D., Jahn, E., Fahlke, B., Ladvig, G., and Haubenreisser, U., *Zeolites* **5**, 53 (1984).
9. Moffat, J. B., *Catal. Rev.-Sci. Eng.* **18**, 199 (1978).
10. Baumgarten, E., and Weinstrauch, F., *Spectrochim. Acta Part A* **35**, 1315 (1979).
11. Paukshtis, E. A., and Yurchenko, E. N., *React. Kinet. Catal. Lett.* **16**, 131 (1981).
12. Little, L. H., "Infrared Spectra of Adsorbed Species." Academic Press, London/New York, 1966.
13. Paukshtis, E. A., Soltanov, R. I., Yurchenko, E. N., and Jiratova, K., *Collect. Czech. Chem. Commun.* **41**, 2044 (1982).
14. Paukshtis, E. A., Soltanov, R. I., and Yurchenko, E. N., *React. Kinet. Catal. Lett.* **16**, 93 (1981).
15. Malysheva, A. V., Theses, Novosibirsk, 1986.
16. Chang, C. D., *Catal. Rev.-Sci. Eng.* **25**, 1 (1983).
17. Trokhimets, A. I., Mardilovich, I. R., Vladyko, L. I., and Garmashev, Yu. M. *Izv. Akad. Nauk BSSR Ser. Khim. Nauk* **2**, 53 (1979).
18. Kikhtyanin, O. V., Ione, K. G., and Mastikhin, V. M., *Chem. Express* **1**, 721 (1986).